



Imaging the Hypoxic Tumor Microenvironment in Cancer Models

15

Arpana Parihar, Palak Sharma, Mrinalini Sharma, and Raju Khan

Abstract

In hypoxic condition oxygen supply is disrupted, and it happens in myocardial infarction, stroke, or tumorous growth. If cells in normal tissue lose their oxygen supply abruptly, they commonly die, while in the tumor, cells become hypoxic over time due to the fast spread of cancer cells that led to deficiency in blood vessels which cause nutrient and O₂ deprivation. Tumor cells acclimatize to these changes by augmenting the production of multiple proteins that enable them to survive. These proteins suppress apoptosis, increase aggressiveness by promoting metastatic spread, switch metabolism from a mitochondria-dependent pathway to glycolysis, and promote the formation of new vasculature. Because of these pathophysiological consequences, patients with hypoxic tumors often have poor prognoses and treatment outcomes. To assess this hypoxic environment thereby improve the treatment efficacies, a number of molecular imaging systems have been progressed for hypoxia diagnostics in patients; these include invasive procedures like the use of oxygen polarographic electrode which measures tissue

A. Parihar (✉)

Industrial Waste Utilization, Nano and Biomaterials, CSIR-Advanced Materials and Processes Research Institute (AMPRI), Bhopal, MP, India

P. Sharma

NIMS Institute of Allied Medical Science and Technology, NIMS University, Jaipur, Rajasthan, India

M. Sharma

Formerly associated with Raja Ramanna Centre for Advanced Technology, Indore, India

R. Khan

Industrial Waste Utilization, Nano and Biomaterials, CSIR-Advanced Materials and Processes Research Institute (AMPRI), Bhopal, MP, India

Academy of Scientific and Innovative Research (AcSIR), Ghaziabad, India

© The Author(s), under exclusive license to Springer Nature Singapore Pte Ltd. 2023

329

S. Mukherjee, J. R. Kanwar (eds.), *Hypoxia in Cancer: Significance and Impact on Cancer Therapy*, https://doi.org/10.1007/978-981-99-0313-9_15

oxygen and phosphorescence quenching, noninvasive techniques such as magnetic resonance imaging (MRI) which detects oxygenation or lactate production, photoacoustic tomography (PAT) which detects sound waves produced by the absorption of light and provides oxygen saturation curve, radionuclide imaging PET (positron emission tomography), SPECT (single-photon emission computed tomography), and so on. This chapter summarizes and discusses currently accessible techniques that can be successfully used for imaging tumors along with the advantages and disadvantages. In addition, a brief insight into the mechanism of hypoxia in tumors has been presented.

Keywords

Tumor imaging · Hypoxia · Tumor microenvironment · HIF · VEGF

15.1 Introduction

Hypoxia is a physiological state marked by insufficient oxygen supply to tissue cells, where hypo refers to “less than the norm” (normal) and oxia refers to “oxygenation.” In tumors, abnormal growth due to uncontrolled proliferation of cells and changes in metabolism lead to deprivation of oxygen demand from the preexisting blood vessels making them more susceptible to hypoxia, especially in the case of malignant solid tumors. In order to adjust to altered conditions, hypoxia-induced adaptive responses include suppression of apoptosis or autophagy and enhancement of angiogenesis. Vasculogenesis and increase in aggressiveness of the tumor, alteration in DNA repair pathways, and change in cellular metabolism also reduce antitumor responses (Ranjan et al. 2020; Parihar et al. 2021a, 2022a, b; Munjal et al. 2022). Besides these cellular adaptive responses influenced by hypoxia, reduced oxygenation in tumor tissue induces chemoresistance by altering drug transport and cellular absorption. The lack of oxygen essential led to the enhancement of cytotoxicity of several chemotherapeutics. Hypoxia also induces resistance to radiation therapy. Thus, knowing the extent and degree of hypoxia is imperative before the instigation of medication. A variety of approaches are being developed to evaluate hypoxia based on measuring oxygen levels in tissues directly or indirectly. Direct techniques include polarographic needle-based electrodes, near-infrared spectroscopy, phosphorescence imaging, blood oxygen-level-dependent imaging, electron paramagnetic resonance imaging, and magnetic resonance imaging. Indirect or noninvasive techniques include the measurement of immunolabeled exogenous and endogenous hypoxia markers, which can provide parameters related to oxygenation. Clinicians have been confronted to develop different treatment strategies. As a result, clinicians designed O₂ concentration measuring devices. Polarographic electrodes directly measure O₂ levels with needle-type probes, both optical and electrochemical. However, various problems obstruct their practical use, and better approaches for correctly detecting tumor hypoxia are entailed for hypoxia prognosis and therapeutic development. Indirect, noninvasive techniques, such as immunolabeling

Imaging the Hypoxic Tumor

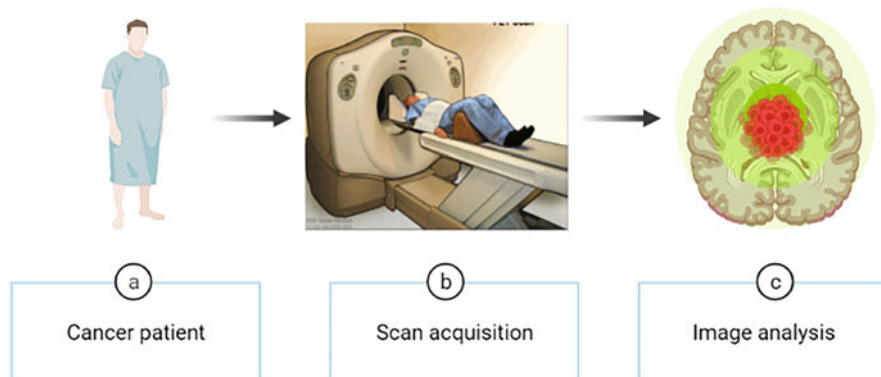


Fig. 15.1 General steps involved in imaging hypoxia tumor. Created with [BioRender.com](https://www.biorender.com)

endogenous or exogenous markers, have also been improved. Researchers have also used fluorescent, phosphorescent, and luminescent reporters to give real-time measurements of O_2 in living cells or tumors. Some modalities such as MRI (magnetic resonance imaging) and PET (positron emission tomography) are often used in medical imaging. Although several techniques for detecting tumor hypoxia use different pathways, very few modalities are licensed for use in clinical practice. The assessment of the extent of tumor hypoxia is a crucial step for the validation and development of treatment targeting hypoxia that will eventually be used in general clinical practice (Walsh et al. 2014; Godet et al. 2022). The general steps involved in imaging hypoxia tumors are shown in Fig. 15.1. The present chapter deals with the tools and techniques available for the measurement of tumor hypoxia along with their pros and cons.

15.2 Mechanism of Hypoxia in Tumors

Hypoxia is a pathological state that is characterized by a low-oxygen tension state. Under ordinary conditions, cells within developing tissue need to be supplied with oxygen. Although the oxygen supply is carefully controlled, there might not always be enough oxygen available. For instance, in a rapidly growing tumor, extreme hypoxia may develop. The core of the tumor has an insufficient supply of oxygen and nutrients which causes cells to become necrotic, while in the outer areas, cells live. Diffusion may provide oxygen to a small tumor with a diameter of lesser than 1 millimeter. The presence of oxygen corresponds to normal tissues. If tumor development persists, the percentage of oxygen in the central area of the tumor drops. When the tumor expands further, the O_2 can drop to below 0.02%, and the tumor cell experiences severe hypoxia. To avoid severe hypoxia and necrosis, tumor

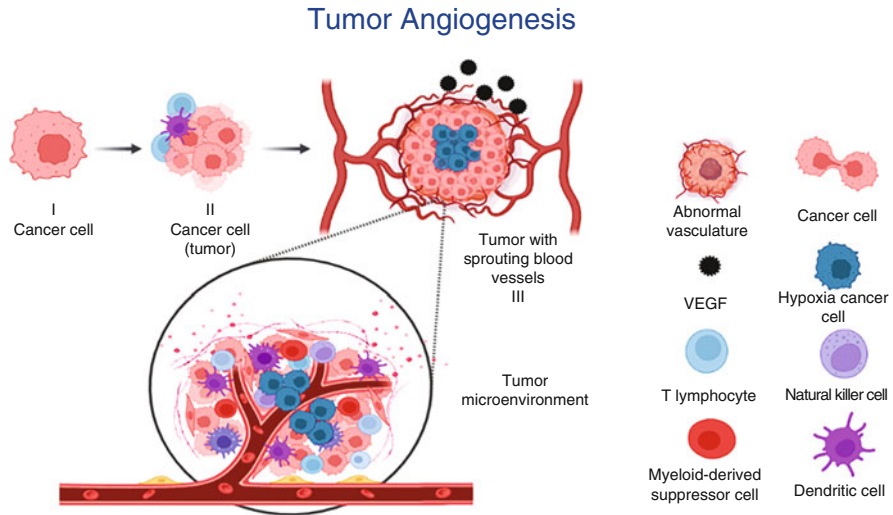


Fig. 15.2 The natural killer cell (NK cell) detects molecules related to stress on damaged cells. Dendritic cells (DC) turn on $CD8^+$ T cells, which then send tumor-corresponding antigens using their receptor. When NK cells and $CD8^+$ T cells are activated, they let out granzymes and perforin. They poke holes in the membrane of the tumor cells, which makes them die through apoptosis, as shown in step II. However, when the tumor progresses, it may not display the chemicals that the immune cells recognize. Additionally, tumors can entice immune cells that inhibit the action of other immune cells, thereby promoting tumor development. These immunosuppressive cells include Tregs and a certain type of myeloid cells; therefore the tumor microenvironment consists of two opposing immune responses: one side of the immune system is attacking the tumor, while the other is helping it to grow, as shown in step III. The image is created with [BioRender.com](https://www.bio-render.com)

may induce the growth of new blood vessels. This sprouting of new vessels from existing blood vessels is called angiogenesis (Weis and Cheresh 2011). The process starts when an small vessel of endothelial cell is activated by an angiogenic stimulus via vascular endothelial growth factor (VEGF) (Melincovici et al. 2018) which is responsible for capillaries sprouting as shown in Fig. 15.2 (Melincovici et al. 2018).

Alternatively, tumor cells may invade surrounding normoxic tissue areas. Angiogenesis, invasive tumor growth, and other adaptive reaction are regulated by the hypoxia-inducible factor, abbreviated HIF. It is a transcription factor consisting of alpha- and beta-subunits. The dimerization of one of the three distinct α -subunits with one of the two different β -subunits occurs. In analogy to the α -subunit, the β -subunit is not receptive to oxygen. Among the α -subunit, the function of HIF-1 α and HIF-2 α is most comprehended. The domain of the HIF-1 α consists of an N-terminal basic helix loop helix (bHLH) motif which correlates with DNA. Two distinct transactivation domains can be found close to the C-terminal. These domains regulate how the HIF-1 α gene is transcribed into mRNA. The helix domain, in addition to the helix loop, is required in dimerization with the HIF β -subunit. The arginine residue (N⁸⁰³) modulates the transcriptional activity, and the proline residues (p⁴⁰² and p⁵⁶⁴) are essential for protein stability. The HIF-2 α contains

domains similar to those in HIF-1 α . The bHLH domain, which is part of the dimerization motif, is found in the HIF-1 β -subunit. The protein contains only one transactivation domain. As mentioned before HIF α -subunit contains prolyl residue which is critical to the stability of the protein. Human tissues primarily contain molecular oxygen levels between 10 and 30 micromolar. Under this normoxic condition, one or both the critical prolyl residue and HIF α proteins will be hydroxylated by a member of the prolyl hydroxylase domain family abbreviated PHD2. PHD2 is the major hydroxylase that hydroxylates HIF α . The PHDs are dioxygenases and contain both molecules of O₂, in their product; also prolyl residues are the substrate of PHD dioxygenases. In the oxidative decarboxylation of α -ketoglutarate (an intermediate of the Krebs cycle), one O₂ atom is utilized. PHD dioxygenases required bivalent iron. The process produces hydroxy prolyl residue, carbon dioxide, and succinate, which is also a Krebs cycle intermediate. The von Hippel-Lindau protein, abbreviated pVHL, binds to HIF α when one or both of the essential prolyl residues are hydroxylated (Hayashi et al. 2019). The VHL gene is a tumor suppressor, which implies that it inhibits excessive or uncontrolled cell growth and division. The VHL protein is attached to the ubiquitin ligase complex, which also comprises cullin, elongin, and ring box protein 1 (ECR). An E2 ubiquitin-conjugating enzyme attaches ubiquitin to HIF α . The 26s proteasome breaks down polyubiquitinated HIF α . The C-terminal transactivation region of the HIF α protein comprises a crucial arginine and prolyl residue. The residue is hydroxylated by a dioxygenase called factor inhibiting HIF-1 α or FIH-1. Similar to the prolyl hydroxylase domain, the FIH-1 contains both molecules of O₂, in its product. The oxidative decarboxylation of alpha-ketoglutarate utilizes a single oxygen atom. The product of the reaction is hydroxy arginine residue, carbon dioxide, and succinate. The hydroxylation of arginine residue inhibits the binding of p300 and CBP transcriptional co-activators. The PHD dioxygenases are unable to hydroxylate HIF α proteins in low-oxygen environments. HIF α -subunit along with a HIF β -subunit binds to consensus sequences in the DNA. The p300 and CBP co-activator bind to HIF-alpha. The complex activates the transcription of the target gene (Burslem et al. 2017; Manuelli et al. 2021). Steps involved in both hypoxic and normoxic conditions are compared in Fig. 15.3.

15.3 Approaches for Imaging Tumor Hypoxia

Researchers are developing many approaches to measure hypoxia within tumors to overcome hypoxia-induced problems and to improve the therapeutic management of cancer. For assessing tumor hypoxia, reliable, noninvasive methods are desirable, so that patients can be selected for therapeutic management according to their needs. Various techniques have been anticipated to assess hypoxia in tumors based on direct or indirect measurements of oxygen concentrations. Tools and techniques which are currently available or under progress for the detection of tumor hypoxia are enlisted in Table 15.1. These are divided into three categories: methods that directly measure oxygen concentration, i.e., invasive methods, approaches that

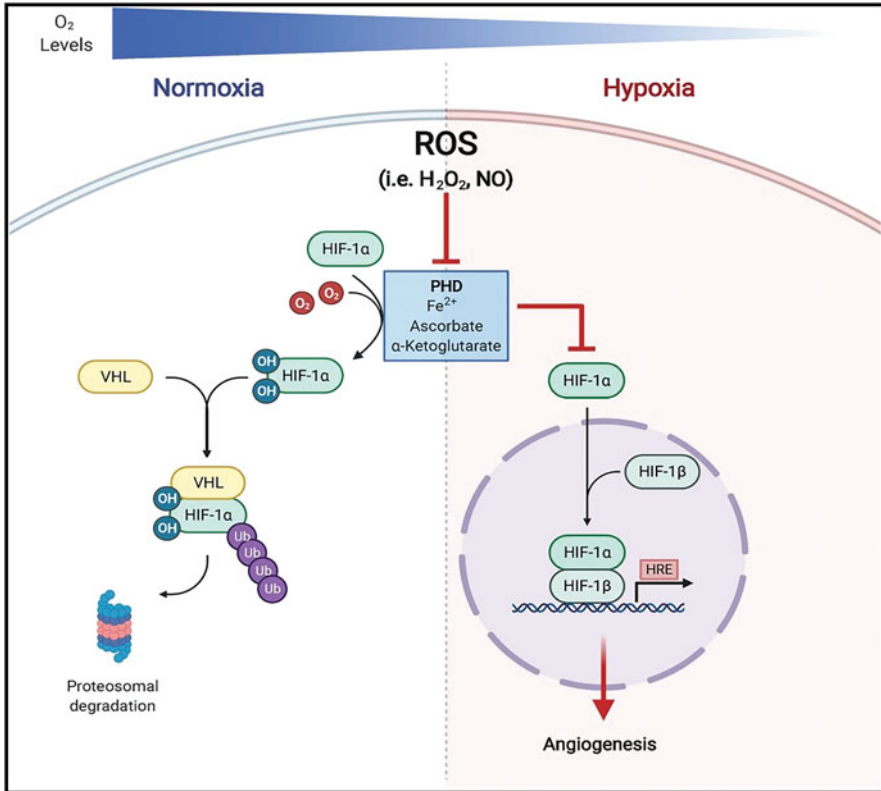


Fig. 15.3 The HIF-1 signaling pathway is represented schematically in normoxic and hypoxic environments. Under normal conditions (left side), PHD hydroxylates HIF-1 α , causing it to interact with VHL. In hypoxia (right side), PHD activity is prohibited, preventing HIF-1 α breakdown due to a deficiency of oxygen and high amounts of ROS (including H₂O₂ and NO). Consequently, HIF-1 α gathers in the cytoplasm before translocating to the nucleus and making a transcriptionally active HIF-1 complex with HIF-1 β . The HIF-1 complex detects and interacts with the hypoxia response element (HRE) sequence, increasing the transcription of HIF-1 targets, comprising those implicated in angiogenesis (reproduced with permission from (Manuelli et al. 2021))

report on physiologic processes involving oxygen molecules, and noninvasive methods that examine endogenous marker expression in response to hypoxia (Sun et al. 2011).

15.3.1 Invasive Approaches

A medical procedure in which the body is penetrated, usually by cutting or puncturing the skin or inserting equipment, is the invasive approach. Different types of invasive approaches for tumor imaging are discussed below.

Table 15.1 Methods currently available or under development for the detection of tumor hypoxia

Sn. no.	Methods	Advantages	Disadvantages	Approved clinical procedure	Ref.
A					
Invasive approaches					
1	Oxygen polarographic electrodes	Gold standard technique	Limited sampling capabilities, highly invasive, measurements can't be repeated, appropriate only for tumors that are easily accessible, with the possibility of altering oxygen concentration	Approved	(Chaplin et al. 2011)
2	Phosphorescence quenching	Oxygen sensing is independent of tracer concentration, has an exceptional temporal resolution, and enables real tissue oxygenation	Decay and photobleaching	Europe only	(Kurokawa et al. 2015)
Endogenous markers associated with hypoxia					
3	Hypoxia-inducible factor-1; carbonic anhydrase IX; glucose transporter 1; osteopontin	Provide primary indication about the cancerous condition	Less specific and the detection limit is moderate	Not approved	(Kudo et al. 2009; Carvalho et al. 2011)
Noninvasive approaches					
4	MRI-BOLD (blood oxygen-level dependent)	There is no O ₂ absorption; higher temporal resolution	Susceptible to disruption; unfavorable for tissue hypoxia	Preclinical	(O'Connor et al. 2019)
5	MRI-TOLD (tissue oxygen-level dependent)	Regardless of perfusion, short acquisition periods, hyperoxic gas challenge, and measurement of hypoxia throughout time	Throughput is relatively low and susceptible to motion artifacts	Preclinical	(Zhang et al. 2014)
6	MRI-fluorine	No oxygen is needed; real-time monitoring	Current clinical equipment is inappropriate	Not approved	(Chapelin et al. 2018)

(continued)

Table 15.1 (continued)

Sn. no.	Methods	Advantages	Disadvantages	Approved clinical procedure	Ref.
7	Near-infrared spectroscopy/tomography	Authorized by doctors for use as pulse oximetry	Low-light attenuation, restricted tissue penetration, and confined to certain body sections	Approved	(Yu 2012)
8	Photoacoustic tomography (PAT)	Provide 3D tomographic images, high spatial resolution (~60 μm), and tissue penetration depth of ~30 cm	Restricted imaging window	Preclinical	(Zhang et al. 2020)
9	Hypoxia PET imaging	Noninvasive; very sensitive; quantitative; evaluation of the entire tumor volume; spatial mapping of hypoxia; repeated evaluation	Inadequate trace; susceptibility to false-positive findings; uptake in normal tissues; inadequate spatial resolution and tumor background ratio	Approved	(Fleming et al. 2015)
10	SPECT (single-photon emission computed tomography)	Noninvasive, tumor diagnosis on a macroscopic scale, high sensitivity, hypoxia detection throughout time	Resolution is restricted; fewer agents are accessible than with PET; it is difficult to measure hypoxia	Preclinical	(Daimiel 2019)

15.3.1.1 Oxygen Polarographic Electrodes

This method is based on the detection of oxygen molecules by electrochemical reduction using a polarographic electrode and is used extensively for measuring oxygen in both human tumors and animal studies. Although, it is a direct approach to determining tissue oxygen content, this approach is sometimes referred to as the “gold standard.” The O_2 assessments entail injecting an electrode in a tumor or invasive lymph node and monitoring O_2 in submillimeter increments from different points per needle track as shown in Fig. 15.4 (Parker et al. 2004; Marland et al. 2020). The more regular the lesion form, the more representative the pO_2 values will be. In most cases, more than a hundred measurements are taken in suitable sites of the lesion, resulting in a composite illustration of the hypoxic condition of the lesion. Although, it is a lengthy procedure, the probes sample a tissue volume of 50–100 cells. Only surface lesions, such as metastatic lymph nodes, are accessible to the polarographic probes and have restricted sampling capacities (Parker et al. 2004).

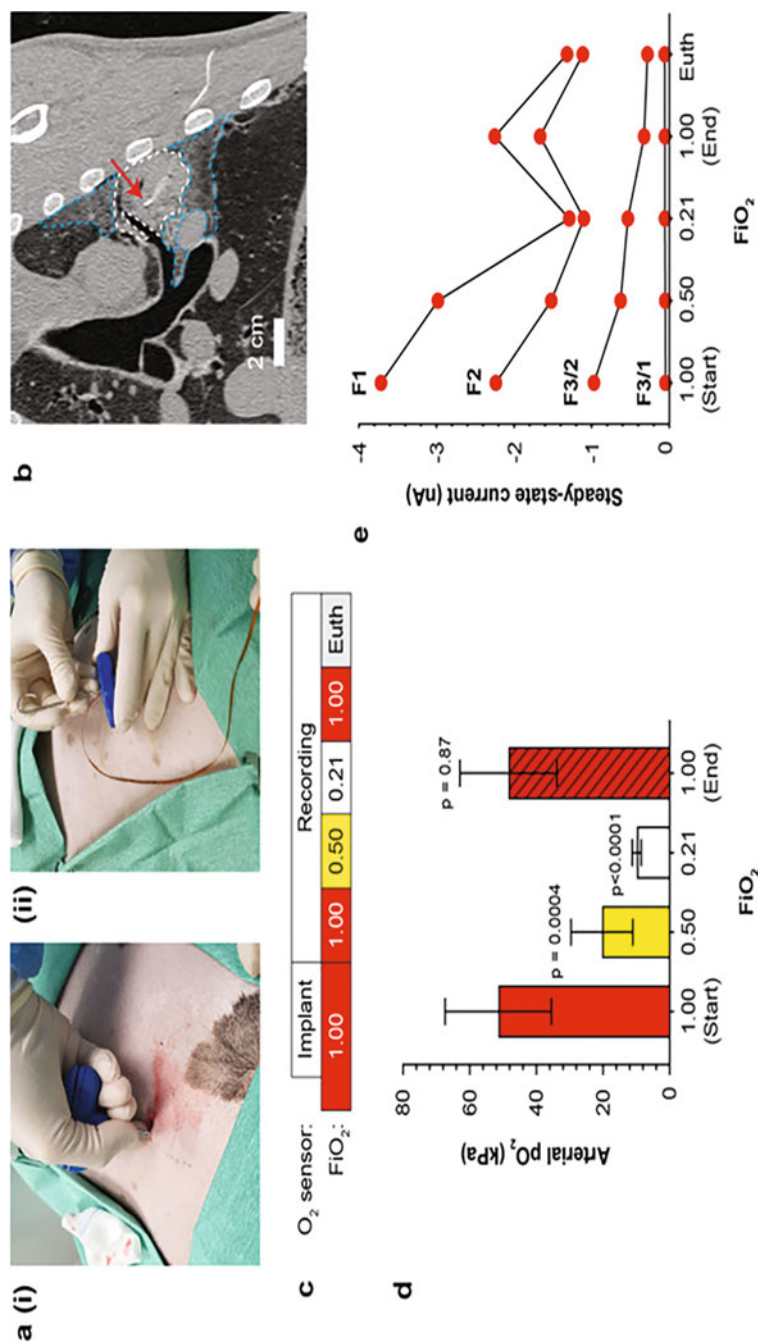


Fig. 15.4 Surgical insertion and sensor operation are conducted on lung tumors. **(a)** Images demonstrating the surgical implantation of a sensor: (1) putting a Jamshidi needle through the chest wall into a lung tumor; (2) insertion of the sensor and lead wire. **(b)** After implantation, a standard thoracic coronal CT scan reveals sensor placement (red arrow) inside tumor tissue. The tumor is encircled by areas that mimic secondary pneumonia or neoplastic foci (blue dashed outline). **(c)** Sensor installation and sequence diagram for FiO₂. **(d)** Arterial blood partial oxygen concentration after every FiO₂ step ($n = 4$ repetitions of the experiment with three animals). The error bars depict the standard deviation between repetitions. **(e)** Typical sensor performance at every FiO₂ concentration over the final 5 mins of the FiO₂ stage. Each sensor's output is shown separately. (Reproduced with permission from (Marland et al. 2020))

For deep-seated tumors and to measure overall oxygen status, a polarographic electrode can be used under guidance CT. In addition, the proportion of pO₂ tension varies minimally between primary tumors and lymph node metastases; thus node measures can be used as surrogates for the underlying tumor's hypoxic condition. Oxygen electrodes have a number of drawbacks that prevent them from being used in clinical practice on a regular basis. The approach is also quite intrusive, making repeat measurements extremely difficult. It is, however, challenging to create 3D oxygen maps using electrodes. Because the probe cannot distinguish between living and dead tissue, the probe exaggerates hypoxia in necrotic areas. When patients are given halogenated anesthetics (such as halothane), polarographic electrodes perform poorly, resulting in erroneous oxygen readings. In addition, the equipment handling needs a technically experienced operator, and inter-operator variance can be considerable.

15.3.1.2 Phosphorescence Quenching

In this technique, oxygen detection is dependent on the interaction between oxygen molecules and phosphorescence dyes. The dyes release their own light when exposed to a brief flash of light, and the intensity of emission decreases exponentially with the surrounding oxygen concentration (Kurokawa et al. 2015). Stern-Volmer constant tissue oxygenation may be assessed using factors such as the decay rate in the absence of oxygen. The advantage of this technique is oxygen measurements are independent of tracer (dye) concentrations as phosphorescence lifetime is measured instead of signal intensity. The decay rate is translated into tissue oxygenation using pre-calibrated factors such as the decay rate in the oxygen-deprived environment and the Stern-Volmer constant. Because phosphorescence duration rather than signal intensity is examined, the oxygen response is unaffected by tracer amount, unlike other oxygen-sensing systems. This high-temporal-resolution technology enables a real-time tissue oxygenation profile that seems to be challenging to get using conventional techniques. Both molecular reporters and physical needle probes have been used to assess oxygen concentration in vivo (Ziemer et al. 2005).

15.3.2 Endogenous Markers of Hypoxia

More recently, molecules involved in hypoxic response of tumor cells are considered as endogenous markers of hypoxia. Several proteins, including the glucose transporter 1 (GLUT1), carbonic anhydrase 9 (CA 9), and hypoxia-inducible factor-1 (HIF-1), can be detected immunohistochemically in archival pathologic substrate and are briefly explained below.

15.3.2.1 Hypoxia-Inducible Factor

HIF-1 α is a transcriptional activator whose activity is controlled by oxygen levels (Ziello et al. 2007). It enhances several metabolic processes targeted at reducing hypoxia's negative impacts. Since it is continuously produced and degraded by

oxidation via oxygen, its deprivation is inhibited under low-oxygen pressure, resulting in elevated protein levels in numerous hypoxic malignancies. HIF-1 α translates tumor hypoxia with several target expressions associated to hypoxia (Hu et al. 2003). Both hypoxia and normoxic signaling pathways are involved in activating HIF-1 α expression in human cancer. When the phosphoinositide 3 kinase (PI3K), Akt, and mammalian target of rapamycin (mTOR) apoptotic pathways are switched on, the HIF-1 gene shoots up. Mutant forms of phosphatase and tensin homolog (PTEN), VHL, fumarate hydratase, or succinate dehydrogenase have also been shown to stimulate HIF-1 transcription (Schönenberger and Kovacs 2015). Growth factors like insulin growth factors and epidermal growth factor aid to maintain protein stability under normoxic conditions. The deposition of HIF-1 α can also be stimulated by the production of mitochondrial ROS which oxidize iron in the active site of PHD, preventing it from hydroxylating HIF-1. HIF-1 α expression is associated with reduced disease-specific survival (DSS) for people with colorectal cancer and gynecological cancer; even so, HIF-1 α expression has been associated with lower disease-specific survival (DSS) in patients with colorectal cancer, and similar results have been found in patients with gynecological cancer (Imamura et al. 2009). Higher levels of HIF-1 α observed in H&NC patients correlate with 5-year DFS in patients who had surgery (Walsh et al. 2014).

15.3.2.2 Carbonic Anhydrase IX

CA-IX (carbonic anhydrase IX) is an enzyme which simulates the reversible modification of bicarbonate anion to CO₂; also when oxygen pressure is less than 20 mmHg, its expression is increased. CA-IX is essential for the acidity of tumors; especially when the oxygen level is low, this can often make it harder for ionizable drugs to function, which is persistent with its function as a pH regulator of tissue. For example, in breast cancer patients receiving doxorubicin treatment, CA-IX expression was observed to be associated with poor progression-free survival (PFS) and overall survival (OS) (Pastorekova and Gillies 2019). Although CA-IX expression in H&NC patients did not have a substantial correlation with pO₂ levels or pimonidazole (PIMO) staining, this advocates that CA-IX expression is associated with factors other than the pO₂ level. Increased amounts of CA-IX protein are attributed to hypoxia in cervix cancers but not in colorectal adenocarcinomas (Pastorekova and Gillies 2019). In addition to its significance in H&NC, CA-IX has also been reported to be a poor factor for survival in non-small cell lung cancer (NSCLC), cervical cancer, and breast cancer. Patients with H&NC having radiotherapy with carbogen and nicotinamide HA are related to CA-IX expression. When a dichotomized cutoff value for low vs high CA-IX expression in sample biopsy was used, high CA-IX expression was associated with higher LRC and free from distant metastases. This is a surprising finding and emphasizes the complicated function of CA-IX expression in cancerous tumors.

15.3.2.3 Glucose Transporter-1

GLUT-1 is a membrane protein that aids in the transport of glucose across cell membranes (Navale and Paranjape 2016). This transporter is upregulated to fulfill

the increased glucose requirement of hypoxia cells, which arises from the increasing glycolysis that takes place under low-oxygen conditions. This protein is found in high concentrations in a variety of tumors, and its overexpression is linked to hypoxia in the head, neck, and cervix tumors. Clinical results deteriorate when this protein is expressed in H&NC and bladder cancer (Pezzuto et al. 2020).

15.3.2.4 Osteopontin

Osteopontin (OPN) belongs to the N-linked glycoprotein family of small integrin-binding ligands. It is secreted as an acidic glycoprotein, phosphorylated and binds with numerous integrins via its arginine-glycine-aspartic acid (RGD) integrin-binding motif. OPN is displayed in several cells, such as macrophages, endothelial cells, and smooth muscle cells, and is engaged in vascular remodeling, cell adhesion, and immune functioning. Hypoxia increases OPN expression via the activation of Akt and activation of the ras-activated enhancer (RAE) in the OPN promoter. Furthermore, in patients with head and neck malignancies, plasma OPN levels have been observed to compare negatively with pO_2 levels. In stage IV head and neck cancer patients, tumor OPN expression was found to be linearly related to median pO_2 levels. OPN promotes integrin and MMP signaling pathways by binding to tumor cell surface receptors, increasing tumor cell invasion, migration, and adhesion.

15.3.2.5 Pimonidazole

PIMO is a lipophilic exogenous hypoxia marker with the hypoxia-targeting 2-nitroimidazole chemotype. PIMO was initially intended as a radiosensitizer and is found to be more effective than misonidazole (MISO); however, it was unsuccessful to validate efficacy in later clinical testing. Currently, PIMO is used as an exogenous hypoxia marker. A few hours before tumor biopsy, PIMO is delivered directly into a vein or orally. Hypoxia in tissue samples can be found with the help of a PIMO metabolite staining kit that uses commercially available antibodies. A high linear correlation ($r^2 = 0.81$) was found between the concentration of PIMO and the amount of oxygen in phantoms and animal tumor models. But there was no correlation between the presence of PIMO in needle biopsies and pO_2 readings in women with uterine cervical cancer.

15.3.3 Noninvasive Approaches

Although the invasive methods and endogenous markers can offer a somewhat precise evaluation of tumor oxygenation, these techniques are biased and reveal partial evidence in the tumor area. Thus, there has been an increase in curiosity in using noninvasive methods. The following part illustrates several noninvasive techniques.

15.3.3.1 MRI-Based Measurements

MRI is a valuable tool for measuring hypoxia. In this approach, fluorocarbon reporter molecules are injected directly into a tumor; the absolute PO_2 may be

detected. The PO_2 measured by this method is consistent with electrodes (presumably interstitial PO_2). The general MRI/PAI imaging techniques have been shown in Fig. 15.5. The ability to assess regional PO_2 maps concurrently at 50–150 individual places is a significant advantage over the electrode method. Furthermore, once the reporter molecule is present, consecutive PO_2 maps may be created to highlight changes in oxygenation in response to therapies, such as hyperoxic gas breathing or vascular targeting drugs. Because of a shortage of human MRI equipment capable of 19F MRI, 19F oximetry measurements in patients have yet to be undertaken (Krohn et al. 2008). A kind of imaging technique called blood oxygen-level-dependent (BOLD) MRI distinguishes between oxy-Hb and paramagnetic deoxy-Hb. $T2^*$ -weighted imaging can identify changes in vascular oxygenation. Its vulnerability to changes in Hb concentration, which can be caused by variations in vascular volume and flow as well as the interconversion of oxy- and deoxyhemoglobin, is one major drawback. Instead of using quantitative measurements, this method provides a qualitative assessment of oxygenation changes (Murata 2007). This method is commonly employed in functional brain mapping, to study variations in blood flow as well as in tumor research. BOLD MRI is especially sensitive to oxygen manipulation therapy wherein hyperoxic gas breathing is used to alleviate hypoxia in conjunction with other therapies.

15.3.3.2 Near-Infrared Spectroscopy/Tomography

Near-infrared spectroscopy (700–900 nm) calculates the Hb/HbO₂ ratio using the absorption band of hemoglobin (Hb) and oxy-hemoglobin (HbO₂). This methodology does not detect oxygen content directly; rather, it translates the Hb/HbO₂ proportion into partial pressure of oxygen by using hemoglobin saturation curves. In clinical applications, one version of this method is routinely utilized for rapid oxygenation analysis using pulse oximetry. Additionally, methods based on the spectroscopic anomalies between Hb and HbO₂ are presented. Diffuse optical tomography, in particular, was utilized to rebuild the 3D oxygen concentration in breast cancer. The technique has minimal tissue invasion and is limited to parts of the body with lower-light diminution (Ali et al. 2004).

15.3.3.3 Photoacoustic Tomography (PAT)

It is an imaging method that provides both functional and anatomical data, while detecting tissue hypoxia noninvasively. PAT is an ultrasonic imaging method that recognizes sound waves produced by light absorption. Thermal elastic expansion occurs inside the tissue as a result of heat produced by the absorbed light. This expansion changes the pressure, and ultrasonic waves travel across the tissue. The ultrasonic source is detected and pinpointed by transducers, resulting in 3D tomographic pictures (Parihar and Dube 2022). PAT measures oxygen content by comparing the endogenous HbO₂ and Hb spectroscopic absorption changes. Derived from their varying response, oxygen saturation (SO₂) curves can give an approximation of how much oxygen is in the blood. PAT is predominantly an ultrasonic method, so it has a high spatial resolution (~60 μm) and can reach about 30 cm into the tissue. One major challenge is that the laser aperture confines the size of the

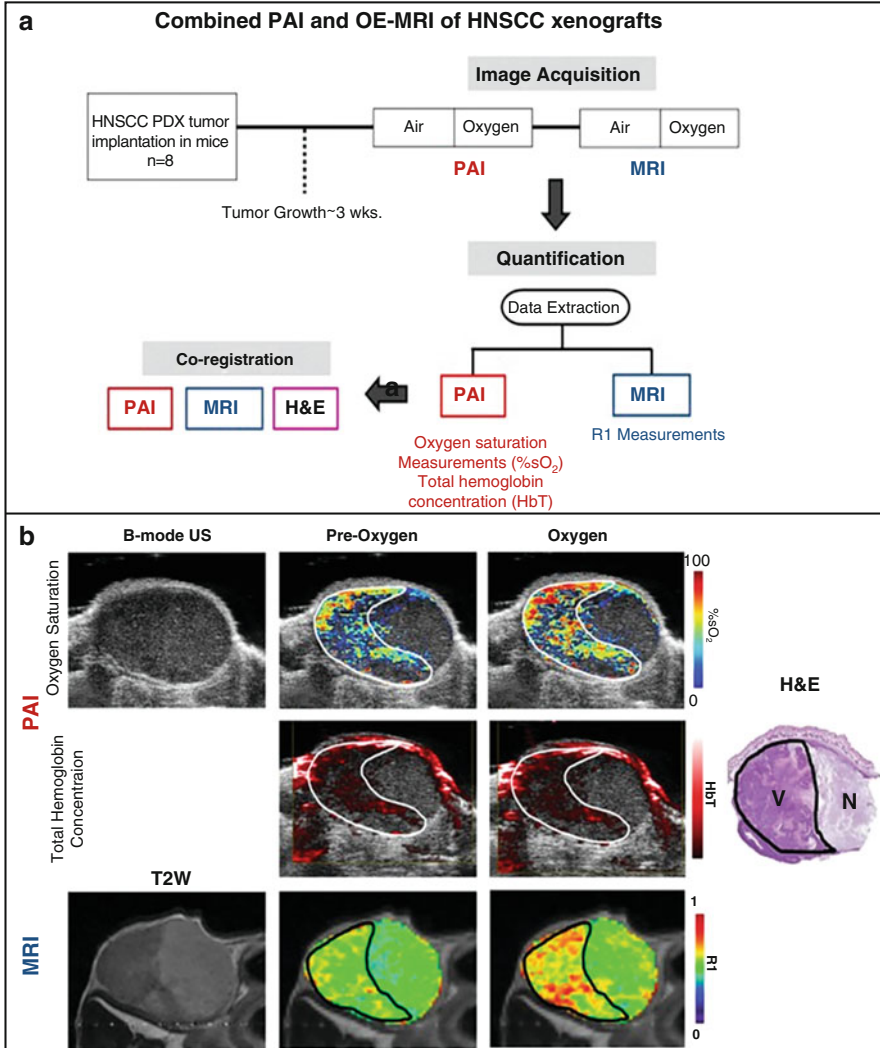


Fig. 15.5 (a) Protocol for MRI, histologic correlation of vascular hemodynamics, and oxygen-enhanced PAI (photoacoustic imaging) in HNSCC xenografts. Mice with tumors were given room air for 2 mins, then 100% oxygen for 6 mins (hyperoxia), before being given room air once more. (b) First row: B-mode PDX-HNSCC oxygen saturation maps in the US and co-registered PA after exposure to room air (pre-oxygen) and then after oxygen (100%; hyperoxia); hemoglobin maps showing the same tumor’s hemoglobin levels before and after an oxygen challenge are shown in the middle row. Last row: the longitudinal relaxation rate (R1) color maps and the axial T2-weighted image of the tumor are shown using the same settings. ((Rich and Seshadri 2016) reprinted with permission)

imaging window. This imaging modality could be used to measure hypoxia because it has a good optical contrast, high structural resolution, and great depth penetration (Xia et al. 2014).

15.3.3.4 Hypoxia PET Imaging

Positron emission tomography (PET) imaging of hypoxia is a noninvasive approach which detects tumor hypoxia using radiolabeled reporters. These tracers are intravenously injected, and their tissue absorption is tracked using a PET camera (Fig. 15.6). However, in hypoxic situations, the lack of oxygen leads to the predominance of a chemically reduced species that localizes inside cells by dechelation or covalent binding to proteins rich in thiols (Xia et al. 2014). These tracers are detected in viable cells but not in dead cells because active enzymes such as cytochromes or nitroreductase are present in living cells to assist the accumulation of radiolabeled metabolites. The absorption of 2-nitroimidazoles and Cu-chelated complexes into hypoxic tissues is sufficient to generate the oxygen saturation necessary for detecting radioresistant hypoxic cells (1% oxygen volume or ~ 7 mmHg of partial oxygen pressure), making them exceptional hypoxia indicators. The selective demarcation of hypoxic cells is facilitated *in vivo* by differences in the absorption and washout of normoxic and hypoxic cells. Biomarkers based on PET provide extensive oxygenation info on tumors, and tests may be repeated. PET imaging using these

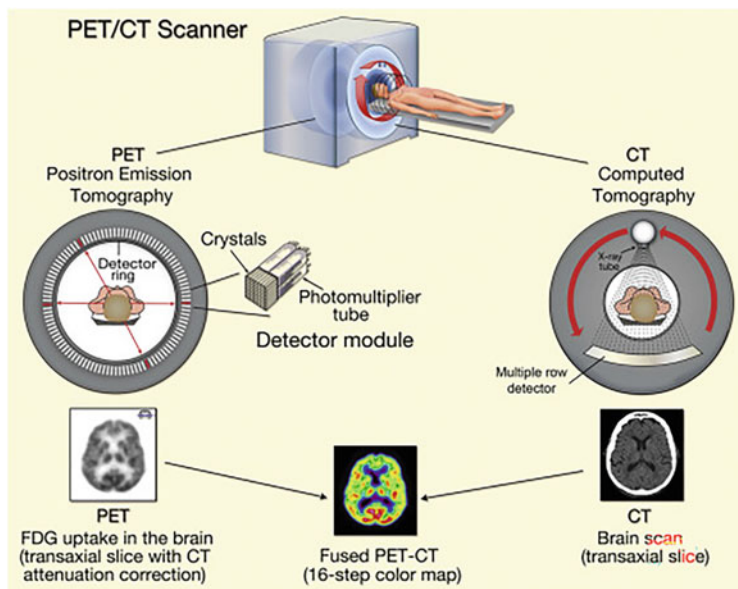


Fig. 15.6 A typical biomedical positron emission tomography (PET) imaging system integrates a cutting-edge PET scanner for molecular imaging. The software and hardware are designed to collect complementing data from a patient bed traveling through both scanners. For PET imaging, the bed slides in gradual increments dependent on the field of view of the PET detectors (usually 16.2 cm), with each acquisition requiring 3–6 mins. (Reproduced with permission from (Lameka et al. 2016))

tracers enables the visualization of the hypoxic condition of the whole tumor and concomitant lesions in metastatic or locally advanced cancer situations, producing a three-dimensional image of hypoxia that electrode- or biopsy-based methods cannot. Due to the relatively low temporal resolution (days between scans), it is not possible to monitor tissue oxygenation in real time. Moreover, since ^{18}F -fluorine has a relatively short half-life ($t_{1/2} = 110$ min), the tracer must be produced and examined in a few hours. For PET imaging, these are the tracers that are used:

- (a) ^{18}F -fluoromisonidazole. The discovery of 2-nitroimidazoles containing radioactive ^{18}F -fluorine atoms for PET imaging of hypoxia was prompted by radiosensitizers of the same chemotype. The radiosensitizer MISO has been radiolabeled as ^{18}F -FMISO. The predominating PET tracer in this class is ^{18}F -FMISO, which has been widely studied for noninvasively detecting hypoxia in vivo via PET imaging. The in vivo bio-distribution pattern of ^{18}F -FMISO is determined by the fact that it is a modestly lipophilic molecule (partition coefficient = 0.40; $\log P = -0.40$). The average amount of ^{18}F -FMISO excreted in urine by individuals is as little as 3% of the total amount administered. In humans, ^{18}F -FMISO is stable in plasma (92–96% intact at 90 mins post-injection) and is typically excreted in the urine as metabolites.
- (b) ^{18}F -fluoroazomycinarabinofuranoside. ^{18}F -fluoroazo-mycinarabinofuranoside (^{18}F -FAZA) is another PET hypoxia imaging agent which is a ribose-containing, hydrophilic (partition coefficient = 1.1) agent with better clearance and hypoxia-targeting characteristics. In preclinical models, ^{18}F -FAZA diffuses into cells quicker than ^{18}F -FMISO and clears from body organs faster than ^{18}F -FMISO. Hepatic metabolism and biliary excretion, as well as urinary excretion, account for the vast majority of the tracer's elimination in humans. Consequently, tracer uptake in the liver, gallbladder, colon, and kidneys is typically moderate to high. While it is hard to determine the extent to which nimorazole mitigated the effects of hypoxia in tumors, the data demonstrate that ^{18}F -FAZA can be utilized to identify patients at risk of failure of treatment.
- (c) ^{18}F -EF5 (pentafluorinated etanidazole). It is the third repetition of the fluorinated "EF" etanidazole by-product and an ^{18}F -radiolabeled analog of the exogenous hypoxia marker EF-5. It is extremely lipophilic (partition coefficient = 5.7) and contains many fluorine atoms (146). The brain is one of the physiological organs where ^{18}F -EF5 has a rapid and homogenous distribution, in contrast to other hypoxia tracers which are intended to have poor lipophilicity. Because of its enhanced lipophilicity, ^{18}F -EF5 has a blood half-life that ranges from 7.5 to 10 h, which exceeds the half-life of ^{18}F -EF3 in blood.
- (d) ^{18}F -HX4 (^{18}F -flortanidazole). With better water solubility and faster background clearance than ^{18}F -FMISO, a newly discovered tracer from the 2-nitroimidazole family was produced, resulting in enhanced pharmacokinetic and tissue clearance characteristics. ^{18}F -HX4 is a water-soluble molecule whose molecular scaffolding contains a polar 1,2,3-triazole element (partition coefficient = 0.21; $\log P = -0.69$). Consequently, the measurement of radiation of ^{18}F -HX4 is equal to ^{18}F -fluorodeoxyglucose (^{18}F -FDG) and ^{18}F -FETNIM; its

bio-distribution is shown not only by lower brain and heart absorption than ^{18}F -FMISO but also by lower GI absorption, permitting imaging in the abdominal region. ^{18}F -HX4 is eliminated from normoxic tissues more promptly than ^{18}F -FMISO, allowing PET imaging to be performed at an earlier stage. Comparable to ^{18}F -FMISO in terms of metabolic stability, it maintains 82% of the tracer in human plasma for 135 mins after delivery.

- (e) Copper (II) (diacetyl-bis(N_4 -methylthiosemicarbazone)). Copper (II) (diacetyl-bis(N_4 -methylthiosemicarbazone)) (Cu-ATSM) is a hypoxia tracer that uses chelated copper ion oxidation/reduction for selective deposition in hypoxic tissue. Copper isotopes that generate positrons have been used: ^{60}Cu ($t^{1/2} = 0.39$ h), ^{61}Cu ($t^{1/2} = 3.33$ h), ^{62}Cu ($t^{1/2} = 0.16$ h), and ^{64}Cu ($t^{1/2} = 12.70$ h). The tracer has undergone in vivo validation and is currently being evaluated in clinical studies. Shorter imaging times (as low as 30 min after injecting) and a high T/B ratio even after its higher lipophilic nature [$\log P = 2.2$ (10)] are Cu-ATSM's primary advantages over 2-nitroimidazole derivatives. The tracer appears to concentrate in the liver of humans, with minimal accumulation recorded in the spleens and kidneys.

15.4 Pits and Falls of Hypoxia Imaging

So far very limited imaging modalities are available to physicians which can diagnose, stage, and treat human cancer: X-ray (computed tomography [CT] and plain film), positron emission tomography (PET), single-photon emission computed tomography (SPECT), ultrasound (US), magnetic resonance imaging (MRI), and optical imaging. Just four of these modalities (CT, SPECT, MRI, and PET) can image cancer in three dimensions in individuals. However, the inception and evolution of these imaging modalities were driven by historical breakthroughs in physics and/or chemistry rather than oncologists' requirements. Because of their inability to scan low numbers of cancer cells, all four 3D imaging methods fall short of tackling many of the complicated clinical concerns associated with cancer screening, staging, and treatment (Parihar et al. 2011, 2013, 2021b).

15.5 Challenges and Future Prospects

The following are some potential future directions for hypoxia imaging and targeted development: since hypoxia targeting is probably worthless in the later stages of cancer, it is crucial to provide solid information that hypoxic cells are therapy determinants in non-SCC and are not merely surrogate signs for severe cancer. Although difficult, such proof may be acquired in rodent research by following a strategy similar to the DAHANCA nimorazole experiments or advanced cell-tagging technologies that allow tracking the postirradiation destiny of tumor cells more directly. Conventional subcutaneous xenograft tumor models made from generations-old cell cultures are inadequate because they can have acquired or lost

certain hypoxia tolerance traits. Orthotopic tumors created using CRISPR/Cas9 *in vivo* gene editing technology and patient-derived xenografts grown directly from tumor biopsies might improve the research and produce more convincing evidence. When selecting illness models and therapy combinations, we must learn from the past to progress in the area of hypoxia targeting and imaging. Overall, the progress of hypoxia-targeting medicines has been dismal. Current preclinical and clinical experiments have been conducted in circumstances where the function of hypoxic cells is ambiguous, which may account for some of the disappointing results. It will be important to better define the nature of the interactions between tumor cells and the related microenvironment during the next 5–10 years. This will be useful in the development of novel cancer therapy techniques that generate a tumor-suppressive phenotype. Furthermore, the identification of novel biomarkers related to tumor stroma may allow for the further delineation of different gene signatures, which may be significant prognostically as well as predict responsiveness to targeted therapy. Successful modulation of angiogenesis in cancer will necessitate a shift from the bench to the bedside and back. Strategies must be examined not only for their impact on tumor development but also on endothelial tip cell sprouting, vascular maturation, endothelial progenitor cell recruitment, hypoxia, and other factors.

15.6 Conclusion

A common biological occurrence in malignant solid tumors, including neck and head, cervical, prostate, breast, and lung malignancies, is tumor hypoxia. Tumor hypoxia spreads irregularly and is not associated with tumor volume, grade, phase, or histopathology. Hypoxic tumors employ a range of survival tactics, which can cause a reduction in apoptotic capability, an elevation in proliferative potential, and the formation of new blood vessels, all of which contribute to an evolutionary selection toward a greater malignant phenotype. As a result, regardless of treatment mode, hypoxia impacts the curability of solid tumors. Given the convincing association between tumor hypoxia and poor treatment results, scientific research has shifted to investigating the efficacy of hypoxia-targeted treatments. Nevertheless, some trials needed a reliable technique for recognizing and selecting patient groups with hypoxic tumors. Thus according to various meta-analyses, the indiscriminate administration of hypoxia modification medication to a patient group with both normoxic and hypoxic cancers exhibited negligible benefits. Hypoxia-based patient lamination has not been employed in medical practice due to the intrusive sort of “gold standard” approach for assessing tumor oxygenation (pO₂ electrode readings). Sponsors are presently faced with the decision of including both tumor types in medical practice, which may dilute efficacy data and jeopardize the trial’s success, or using an unapproved diagnostic technology (e.g., hypoxia PET imaging, MRI, etc.) to identify person with hypoxic tumors. This scenario makes the medical advances of hypoxia-based treatments difficult. Various studies, particularly secondary analyses from bigger trials, demonstrate that hypoxia evaluation predicts tumor grade, therapy response and can recognize high-risk person who requires therapy.

References

- Ali JH, Wang WB, Zevallos M, Alfano RR (2004) Near infrared spectroscopy and imaging to probe differences in water content in normal and cancer human prostate tissues. *Technology in Cancer Research and Treatment* 3:491–497. <https://doi.org/10.1177/153303460400300510>
- Burslem GM, Kyle HF, Nelson A et al (2017) Hypoxia inducible factor (HIF) as a model for studying inhibition of protein-protein interactions. *Chem Sci* 8:4188–4202. <https://doi.org/10.1039/C7SC00388A>
- Carvalho KC, Cunha IW, Rocha RM et al (2011) GLUT1 expression in malignant tumors and its use as an immunodiagnostic marker. *Clinics* 66:965. <https://doi.org/10.1590/S1807-59322011000600008>
- Chapelin F, Capitini CM, Ahrens ET (2018) Fluorine-19 MRI for detection and quantification of immune cell therapy for cancer. *J Immunother Cancer* 6:105. <https://doi.org/10.1186/S40425-018-0416-9>
- Chaplin DJ, Collingridge DR, Young WK et al (2011) Measurement of tumor oxygenation: a comparison between needle electrodes and a time-resolved Polarographic luminescence-based optical sensor. *Radiat Res* 147:329–334
- Daimiel I (2019) Insights into hypoxia: non-invasive assessment through imaging modalities and its application in breast cancer. *J Breast Cancer* 22:155–171
- Fleming IN, Manavaki R, Blower PJ et al (2015) Imaging tumour hypoxia with positron emission tomography. *Br J Cancer* 112:238. <https://doi.org/10.1038/BJC.2014.610>
- Godet I, Doctorman S, Wu F, Gilkes DM (2022) Detection of hypoxia in cancer models: significance, challenges, and advances. *Cell* 11. <https://doi.org/10.3390/CELLS11040686>
- Hayashi Y, Yokota A, Harada H, Huang G (2019) Hypoxia/pseudohypoxia-mediated activation of hypoxia-inducible factor-1 α in cancer. *Cancer Sci* 110:1510–1517. <https://doi.org/10.1111/CAS.13990>
- Hu C-J, Wang L-Y, Chodosh LA et al (2003) Differential roles of hypoxia-inducible factor 1 α (HIF-1 α) and HIF-2 α in hypoxic gene regulation. *Mol Cell Biol* 23:9361–9374. <https://doi.org/10.1128/mcb.23.24.9361-9374.2003>
- Imamura T, Kikuchi H, Herraiz MT et al (2009) HIF-1 α and HIF-2 α have divergent roles in colon cancer. *Int J Cancer* 124:763–771. <https://doi.org/10.1002/ijc.24032>
- Krohn KA, Link JM, Mason RP (2008) Molecular imaging of hypoxia. *J Nucl Med* 49:129–148. <https://doi.org/10.2967/jnumed.107.045914>
- Kudo T, Ueda M, Kuge Y et al (2009) Imaging of HIF-1-active tumor hypoxia using a protein effectively delivered to and specifically stabilized in HIF-1-active tumor cells. *J Nucl Med* 50:942–949. <https://doi.org/10.2967/JNUMED.108.061119>
- Kurokawa H, Ito H, Inoue M et al (2015) High resolution imaging of intracellular oxygen concentration by phosphorescence lifetime. *Sci Rep* 5:1–3. <https://doi.org/10.1038/srep10657>
- Lameka K, Farwell MD, Ichise M (2016) Positron emission tomography, 1st edn. Elsevier B.V
- Manuelli V, Pecorari C, Filomeni G, Zito E (2021) Regulation of redox signaling in HIF-1-dependent tumor angiogenesis. *FEBS J*. <https://doi.org/10.1111/FEBS.16110>
- Marland JRK, Gray ME, Dunare C et al (2020) Real-time measurement of tumour hypoxia using an implantable microfabricated oxygen sensor. *Sensing and Bio-Sensing Research* 30:12. <https://doi.org/10.1016/j.sbsr.2020.100375>
- Melincovici CS, Boşca AB, Şuşman S et al (2018) Vascular endothelial growth factor (VEGF) – key factor in normal and pathological angiogenesis. *Romanian J Morphol Embryol* 59:455–467
- Munjal A, Khandia R, Paladhi S et al (2022) Evaluating the effects of hypotensive drug valsartan on angiogenesis and associated breast ductal carcinoma cell metastasis. *Int J Pharmacol* 18:817–825. <https://doi.org/10.3923/IJP.2022.817.825>
- Murata Y (2007) Comparison of blood-oxygen-level-dependent functional magnetic resonance imaging and near-infrared spectroscopy recording during functional brain activation in patients with stroke and brain tumors. *J Biomed Opt* 12:062110. <https://doi.org/10.1117/1.2823036>

- Navale AM, Paranjape AN (2016) Glucose transporters: physiological and pathological roles. *Biophys Rev* 8:5–9. <https://doi.org/10.1007/s12551-015-0186-2>
- O'Connor JPB, Robinson SP, Waterton JC (2019) Imaging tumour hypoxia with oxygen-enhanced MRI and BOLD MRI. *Br J Radiol* 92:20180642. <https://doi.org/10.1259/BJR.20180642>
- Parihar A, Dube A (2022) Structural alterations in cell organelles induced by photodynamic treatment with chlorin p6-histamine conjugate in human oral carcinoma cells probed by 3D fluorescence microscopy. *Luminescence*. <https://doi.org/10.1002/BIO.4307>
- Parihar A, Dube A, Gupta PK (2011) Conjugation of chlorin p 6 to histamine enhances its cellular uptake and phototoxicity in oral cancer cells. *Cancer Chemother Pharmacol* 68:359. <https://doi.org/10.1007/s00280-010-1492-9>
- Parihar A, Dube A, Gupta PK (2013) Photodynamic treatment of oral squamous cell carcinoma in hamster cheek pouch model using chlorin p6-histamine conjugate. *Photodiagn Photodyn Ther* 10:79–86. <https://doi.org/10.1016/j.PDPDT.2012.05.005>
- Parihar A, Jain S, Parihar DS et al (2022a) Biomarkers associated with different types of cancer as a potential candidate for early diagnosis of oncological disorders. In: *Biosensor based advanced cancer diagnostics*. Academic Press, pp 47–57. <https://doi.org/10.1016/B978-0-12-823424-2.00007-7>
- Parihar A, Malviya S, Khan R (2021a) Identification of biomarkers associated with cancer using integrated bioinformatic analysis. *Cancer Bioinform*. <https://doi.org/10.5772/INTECHOPEN.101432>
- Parihar A, Shrivastava R, Dube A (2021b) Interaction of Cp6-his and Cp6 with bovine serum albumin and liver microsomes: spectroscopic and molecular docking studies. *J Photochem Photobiol* 5:100013. <https://doi.org/10.1016/J.JPAP.2020.100013>
- Parihar A, Singhal A, Kumar N et al (2022b) Next-generation intelligent MXene-based electrochemical Aptasensors for point-of-care cancer diagnostics. *Nano-Micro Letters* 14:1–34. <https://doi.org/10.1007/S40820-022-00845-1>
- Parker C, Milosevic M, Toi A et al (2004) Polarographic electrode study of tumor oxygenation in clinically localized prostate cancer. *Int J Radiat Oncol Biol Phys* 58:750–757. [https://doi.org/10.1016/S0360-3016\(03\)01621-3](https://doi.org/10.1016/S0360-3016(03)01621-3)
- Pastorekova S, Gillies RJ (2019) The role of carbonic anhydrase IX in cancer development: links to hypoxia, acidosis, and beyond. *Cancer Metastasis Rev* 38:65–77. <https://doi.org/10.1007/s10555-019-09799-0>
- Pezzuto A, D'Ascanio M, Ricci A et al (2020) Expression and role of p16 and GLUT1 in malignant diseases and lung cancer: a review. *Thoracic Cancer* 11:3060–3070. <https://doi.org/10.1111/1759-7714.13651>
- Ranjan P, Parihar A, Jain S et al (2020) Biosensor-based diagnostic approaches for various cellular biomarkers of breast cancer: a comprehensive review. *Anal Biochem* 610:113996. <https://doi.org/10.1016/j.ab.2020.113996>
- Rich LJ, Seshadri M (2016) Photoacoustic monitoring of tumor and normal tissue response to radiation. *Sci Rep* 6:1–10. <https://doi.org/10.1038/srep21237>
- Schönenberger MJ, Kovacs WJ (2015) Hypoxia signaling pathways: modulators of oxygen-related organelles. *Front Cell Develop Biol* 3. <https://doi.org/10.3389/fcell.2015.00042>
- Sun X, Niu G, Chan N et al (2011) Tumor hypoxia imaging. *Mol Imaging Biol* 13:399–410. <https://doi.org/10.1007/s11307-010-0420-z>
- Walsh JC, Lebedev A, Aten E et al (2014) The clinical importance of assessing tumor hypoxia: relationship of tumor hypoxia to prognosis and therapeutic opportunities. *Antioxid Redox Signal* 21:1516. <https://doi.org/10.1089/ARS.2013.5378>
- Weis SM, Cheresch DA (2011) Tumor angiogenesis: molecular pathways and therapeutic targets. *Nat Med* 17:1359–1370. <https://doi.org/10.1038/nm.2537>
- Xia J, Yao J, Wang LV (2014) Photoacoustic tomography: principles and advances. *Prog Electromagn Res* 147:1–22. <https://doi.org/10.2528/PIER14032303>
- Yu G (2012) Near-infrared diffuse correlation spectroscopy in cancer diagnosis and therapy monitoring. *J Biomed Opt* 17:010901. <https://doi.org/10.1117/1.JBO.17.1.010901>

- Zhang J, Duan F, Liu Y, Nie L (2020) High-resolution photoacoustic tomography for early-stage cancer detection and its clinical translation. *Radiology: imaging. Cancer* 2:10.1148/RYCAN.2020190030/ASSET/IMAGES/LARGE/RYCAN.2020190030.FIG6.JPEG
- Zhang Z, Hallac RR, Peschke P, Mason RP (2014) A noninvasive tumor oxygenation imaging strategy using magnetic resonance imaging of endogenous blood and tissue water. *Magnetic Resonance Med* 71:561. <https://doi.org/10.1002/MRM.24691>
- Ziello JE, Jovin IS, Huang Y (2007) Hypoxia-inducible factor (HIF)-1 regulatory pathway and its potential for therapeutic intervention in malignancy and ischemia. *Yale J Biol Med* 80:51
- Ziemer LS, Lee WMF, Vinogradov SA et al (2005) Oxygen distribution in murine tumors: characterization using oxygen-dependent quenching of phosphorescence. *J Appl Physiol* 98: 1503–1510. <https://doi.org/10.1152/JAPPLPHYSIOL.01140.2004/ASSET/IMAGES/LARGE/ZDG0040537471004.JPEG>